

RESEARCH ARTICLE | OCTOBER 15 1992

Laser-induced interaction of ammonia with GaAs(100). I. Dissociation and nitridation

X.-Y. Zhu; M. Wolf; T. Huett; J. M. White



J. Chem. Phys. 97, 5856–5867 (1992)

<https://doi.org/10.1063/1.463745>



View
Online



Export
Citation

CrossMark

Boost Your Optics and
Photonics Measurements

Lock-in Amplifier

Zurich
Instruments

Find out more

Boxcar Averager

Laser-induced interaction of ammonia with GaAs(100). I. Dissociation and nitridation

X.-Y. Zhu, M. Wolf, T. Huett, and J. M. White

Department of Chemistry and Biochemistry, Center for Materials Chemistry, University of Texas, Austin, Texas 78712

(Received 13 May 1992; accepted 6 July 1992)

UV laser irradiation of ammonia adsorbed on GaAs(100) leads to molecular desorption and dissociation. A nitride passivation layer can be formed on the GaAs surface at 100 K by simultaneous exposure to ammonia and uv photons in a UHV environment. The nitride layer consists of a mixture of Ga and As nitrides. While the dominating GaN surface species is thermally stable, AsN desorbs below 800 K. Surface NH₂ is identified as an intermediate. The implication of this study for selective area passivation and GaN growth is discussed.

I. INTRODUCTION

Developing GaAs as the next-generation semiconductor material is of great interest because it promises many advantages over Si, e.g., higher performance speed, lower energy consumption, and easier integration of optoelectronic components. A significant problem for GaAs structure is the difficulty of growing dielectric interfaces for metal-insulator-semiconductor (MIS) devices. Unlike Si, where the oxidation process leaves negligible numbers of unsaturated bonds at the Si-SiO₂ interface,¹ oxidation of GaAs usually results in a high density of interface traps near the middle of the band gap.² Since the concentration of defect chemical bonds at the interface is an important figure-of-merit for device performance, passivation of the semiconductor surface, e.g., nitridation, becomes a critical step in device fabrication.³

Nitridation is known to be beneficial in GaAs device fabrication,⁴ particularly in reducing diode leakage currents.⁵ Past attempts to grow nitride passivation layers usually involved exposing GaAs at elevated temperatures (~500 °C) to activated N sources, e.g., a nitrogen plasma.⁶ This process leads to a disordered surface, consisting of mixtures of Ga nitride (GaN) and various volatile As nitrides. Low temperature nitridation with ammonia, using white light synchrotron radiation, showed the growth of similar nitride films on GaAs.⁷ In addition to these efforts, epitaxial growth of single crystal GaN on GaAs substrates has also been successfully demonstrated from molecular beam epitaxy (MBE) or organometallic chemical vapor deposition (OMCVD) using hydrazine or dimethylhydrazine as the nitrogen source.⁸

In this study, we describe a novel low-temperature nitridation process involving the simultaneous exposure of the GaAs(100) surface to ammonia and uv photons in a UHV environment. The (100) surface is chosen because of its technological importance. This laser-assisted nitridation process is the result of nonthermal dissociation of *adsorbed* ammonia. This work has potential technological implications for selective-area passivation of GaAs surfaces, as well as enhanced growth of GaN at low temperatures. At present, GaN films are usually grown with OMCVD using,

e.g., ammonia and trimethylgallium at ~1000 °C.⁹ The high-temperature requirement for conventional GaN OMCVD usually leads to undesirable high *n*-type carrier concentration, resulting from nitrogen vacancies.¹⁰

This is part I of two papers describing uv laser induced interaction of ammonia with the GaAs surface. The companion paper (II) is devoted to the dynamics of molecular ammonia photodesorption.

II. EXPERIMENT

All experiments were conducted in a two-level UHV chamber, pumped by ion, turbomolecular, and Ti sublimation pumps, with a working pressure of $\leq 2 \times 10^{-10}$ Torr. The lower level houses a LK-2000 high-resolution electron-energy-loss spectrometer (HREELS) for vibrational spectroscopy, and the upper level consists of a UTI-100C quadrupole mass spectrometer (QMS), a Perkin-Elmer x-ray photoelectron spectrometer (XPS), and a Phi low-energy electron diffraction (LEED) apparatus. The QMS can be used for temperature-programmed desorption (TPD), and in combination with a multichannel scaler, for time-of-flight (TOF) measurements. The sample holder was mounted on an XYZ manipulator with two rotational stages. The first rotational stage allows the sample to be transferred to various focal points 2.5 in. away from the center axis of the chamber, while the second allows rotation of the sample around an axis containing the sample front face.

The uv light source was a pulsed (11–20 ns) excimer laser (Questec 2110). When filled with different gas mixtures, the laser outputs light at 193 (ArF), 248 (KrF), and 351 nm (XeF). After passing through a series of prisms and apertures, the uv light entered the chamber through a CaF₂ window, uniformly illuminating, along the surface normal, the whole front surface of the sample. To prevent desorption due to thermal heating, the laser pulse energy was kept below 1 mJ/cm², unless otherwise noted. This assured that the calculated transient surface temperature rise during irradiation was no more than a few Kelvin (no temperature rise was detected by the thermocouple). The

reflected light exited the UHV chamber through the entrance window.

The GaAs(100) substrate was a rectangular slice ($15 \times 10 \times 1$ mm) of a semiinsulating wafer (10^{15} cm^{-3} Si-doped). It was held by the edges with two Ta clips which were spotwelded to two Mo leads. The latter were connected to electrically isolated copper blocks which were attached to the manipulator. The temperature was measured by a chromel–alumel thermocouple spotwelded to a small Ta clip which was glued to the bottom edge of the sample with a high-temperature cement (Aremco-571). The substrate could be cooled by liquid nitrogen to 102 K and resistively heated through a 4000 \AA Ta backing to 900 K. Cleaning of the sample was achieved by Ar ion sputtering, annealing (773 K), and flashing (823 K) cycles. Surface cleanliness was verified by XPS and LEED. The latter showed a (4×6) LEED pattern, which corresponds to a Ga-rich ($\sim 70\%$ Ga) surface.¹¹ To minimize adsorption on surfaces other than the sample, ammonia was dosed using a known pressure behind a 2μ pinhole connected to a 8 mm diameter tube that terminated about 2 mm from the GaAs surface (held at 102 K). In nitridation experiments (see Figs. 1–6), the doser tube was 8 mm from the GaAs surface, with both the molecular flux and the laser light incident at 60° , with respect to the surface normal.

All HREEL spectra were taken at 102 K with a primary electron energy of 3 eV and a resolution (FWHM) of $60\text{--}70 \text{ cm}^{-1}$. Both the incident and detection angles were 60° with respect to the surface normal. XP spectra ($\text{Mg K}\alpha$ x-rays; $h\nu = 1253.6 \text{ eV}$) were taken at 102 K with a normal takeoff angle. Typical data averaging time ranges from 2 to 30 min. The spectra were fit and deconvoluted using a mixed Gaussian–Lorentzian function. For a single, well-resolved XPS peak, e.g., $N(1s)$ from 0.5 ML NH_3 on GaAs(100) (see Fig. 1), the fitting was done with four parameters: intensity, position, width, and a shape parameter which determines the relative weight of Gaussian to Lorentzian. The last two parameters were subsequently fixed in the deconvolution of multiple peaks, e.g., $N(1s)$ from mixtures of NH_3 , NH_2 , and GaN (see Fig. 1). TPD experiments (temperature ramp of 7 K/s) were done with the sample in line of sight and 7 cm away from the QMS ionizer. The latter was covered by a shroud with a mesh-covered 6 mm i.d. entrance aperture. This setup, and low ionizer emission current, was employed to reduce electron-stimulated damage of the adsorbates. Over the time required for one experiment, electron-stimulated changes were not detectable.

III. RESULTS

The results will be presented in five sections: Section III A demonstrates the laser-assisted growth of a nitride passivation layer on GaAs(100); Sec. III B probes the structure and thermal reactivity of this nitride layer; Sec. III C presents quantitative calculation of surface coverages from XPS measurements. In an attempt to understand the mechanism of laser-assisted nitridation, Secs. III D and

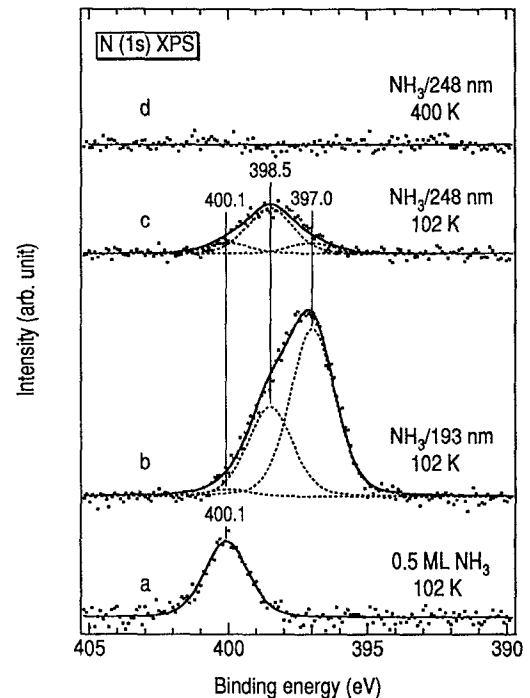


FIG. 1. $N(1s)$ x-ray photoelectron spectra (XPS, $\text{Mg K}\alpha$, 1253.6 eV) taken at 102 K for (a) 0.5 ML NH_3 on GaAs(100)– (4×6) at 102 K; (b) the GaAs(100)– (4×6) surface exposed to NH_3 ($\sim 1 \times 10^{14}$ molecules/ $\text{cm}^2 \text{ s}$) and 193 nm light (5 mJ/cm^2 pulse, 50 Hz) for 60 min at 102 K; (c) and (d) the GaAs surface exposed to NH_3 ($\sim 1 \times 10^{14}$ molecules/ $\text{cm}^2 \text{ s}$) and 248 nm light (5 mJ/cm^2 pulse, 50 Hz) for 60 min at 102 and 400 K, respectively. The solid curves are overall fits to the experimental data (dots) while dashed curves are deconvoluted peaks (see text). The data averaging time was 30 min for each spectrum.

III E concentrate on the photolysis of preadsorbed monolayer ammonia on GaAs(100)– (4×6) .

A. Surface nitride formation

As demonstrated below, a surface nitride layer can be formed by simultaneously exposing a GaAs(100)– (4×6) surface to a NH_3 flux ($\sim 1 \times 10^{14}$ molecules $\text{cm}^{-2} \text{ s}^{-1}$) and a uv photon flux. The resulting surface was then analyzed by XPS, HREELS, TPD, and LEED. We first present XPS results. Figure 1 shows a set of $N(1s)$ XP spectra taken at 102 K. In these, the clean surface spectrum, which showed some broad features from substrate Auger transitions, has been subtracted. The remaining secondary electron background in each spectrum was subtracted using a smoothed step-function fit to the binding energy (BE) region above and below the peak. The resulting spectra are shown as dots in Fig. 1. For reference, spectrum (a) shows saturation NH_3 on GaAs(100) at 102 K. The data (dots) can be fit nicely with a single mixed-Gaussian–Lorentzian function (solid line) peaked at 400.1 eV, as expected for molecular ammonia,^{12,13} with a FWHM of 1.9 eV. Heating to above 350 K eliminates the $N(1s)$ XPS peak, i.e., no thermal decomposition, in agreement with TPD and HREELS results presented below. Based on the relative intensities of $N(1s)$ and substrate Ga ($2p$) transitions, the absolute coverage of saturation am-

monia on GaAs(100)-(4×6) was calculated to be 0.5 ± 0.1 ML or $3.2 \pm 0.6 \times 10^{14}$ molecules cm^{-2} . Details of the calibration procedure for the coverages presented in this figure are presented in Sec. III C.

After the GaAs(100)-(4×6) surface is exposed to NH_3 ($\sim 10^{14}$ molecules $\text{cm}^{-2} \text{s}^{-1}$) and 6.4 eV photons (193 nm) (5×10^{15} photons cm^{-2} , 50 Hz) at 102 K for 60 min, XPS shows a broader N (1s) peak at lower BE (spectrum b). Assuming that this spectrum consists of individual N species with the same FWHM (1.9 eV), the data (dots) can be deconvoluted into mainly two peaks with binding energies at 398.5 and 397.0 eV, respectively. Comparing this to literature values of surface nitrides and NH_x ($x=1,2$) species, we assign the first peak at 397.0 eV to surface GaN (1.1 ± 0.2 ML) and the second peak at 398.5 eV to NH_x ($x=1,2$) and surface As nitride species (0.6 ± 0.1 ML). For example, the N (1s) binding energies for NH_x ($x=1,2$) species on silicon surfaces are at 398.5 ± 0.1 eV,^{13(b)} while those for surface nitrides are at 397.4–397.7 eV on silicon surfaces^{12,13} and 396.6 eV on metal surfaces.¹⁴ The N (1s) BE for GaN on GaAs(100) is between the reported values for silicon and metal surfaces, as would be expected for the difference in electronegativities. Based on the same argument, the N (1s) BE for surface As nitride should be above 397.0 eV, but cannot be resolved from NH_x ($x=1,2$) by the deconvolution method. The intensity of molecular NH_3 at 400.1 eV in spectrum (b) is negligible. Since the starting surface is Ga rich, it is sensible that the surface nitride layer consists of mainly GaN, as observed in nitrogen plasma treatment.⁶ Further support for the above assignments is presented below (see Figs. 2–6).

Spectrum (b) was taken after the GaAs(100)-(4×6) surface was exposed to the indicated NH_3 and 6.4 eV photon fluxes for 60 min. We have also taken XP spectra (not shown) after 30 and 120 min exposure, respectively. While from 30 to 60 min, the N (1s) peak area increased by $\sim 60\%$, further increase in exposure time from 60 to 120 min only leads to $\sim 10\%$ uptake of additional N species. This indicates that the rate of photon-assisted nitridation decreases significantly with the extent of surface nitridation. Although, due to the limitation of UHV conditions, we did not study the nitridation rate beyond 120 min exposure to NH_3 and uv photons, it would be interesting to do similar experiments at much higher NH_3 fluxes.

Changing the energy of uv photons, spectrum (c) shows the N (1s) XPS peak taken after the GaAs(100)-(4×6) surface is exposed to NH_3 ($\sim 10^{14}$ molecules $\text{cm}^{-2} \text{s}^{-1}$) and 5.0 eV photons (248 nm) (1.5×10^{16} photons cm^{-2} , 50 Hz) at 102 K for 60 min. The spectrum can again be deconvoluted to three components at 400.1, 398.5, and 397.0 eV for NH_3 , NH_x/AsN , and GaN, respectively. Compared to spectrum (b) at $h\nu=6.4$ eV, the photon-assisted adsorption rate of N-containing species is apparently lower at $h\nu=5.0$ eV. Unlike spectrum (b), the dominant surface species in spectrum (c) is not GaN at 397.0 eV, but NH_x ($x=1,2$) and/or AsN at 398.5 eV. HREELS analysis confirms that the dominating surface species is NH_2 (see below). Similar results are obtained at $h\nu=3.5$ eV. Since the uv absorbance thresholds of

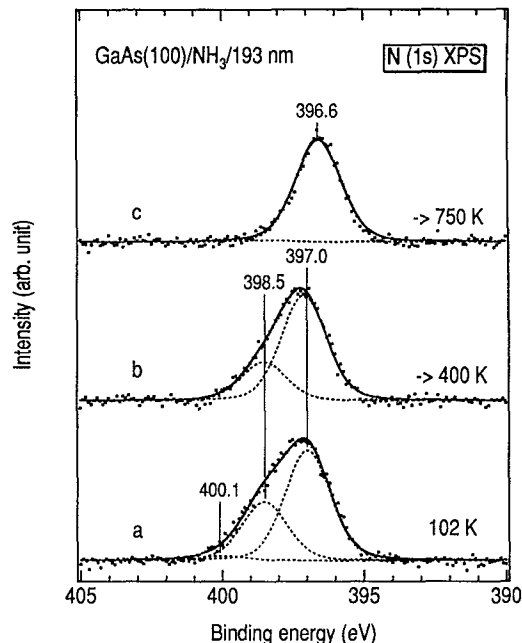


FIG. 2. N(1s) x-ray photoelectron spectra (XPS) taken at 102 K after the GaAs(100)-(4×6) surface was exposed to NH_3 ($\sim 1 \times 10^{14}$ molecules/ $\text{cm}^2 \text{s}$) and 193 nm light ($5 \text{ mJ}/\text{cm}^2$ pulse, 50 Hz) for 60 min at 102 K (a) and heated to 400 K (b) and 750 K (c), respectively. The solid curves are overall fits to the experimental data (dots) while dashed curves are deconvoluted peaks (see text).

gas and condensed-phase ammonia are at $h\nu=5.7$ and 6.2 eV, respectively,¹⁵ the observation of photoassisted nitridation and NH_x formation at $h\nu \leq 5.0$ eV clearly demonstrates that the photoactivation step is not in the gas phase, but in the *adsorbate* state. To further address this point, we examine the effect of substrate temperature on the rate of nitridation.

Spectrum (d) shows the N (1s) BE region obtained after the GaAs(100)-(4×6) surface is exposed to the same photon and NH_3 fluxes as in spectrum (c), but at a higher substrate temperature, 400 K. This temperature is above the thermal desorption temperature of chemisorbed NH_3 , but below those for the reaction-desorption of surface nitrides and NH_x ($x=1,2$) species (see below, Figs. 7, 10, and 11). Within signal-to-noise, no N-containing species were observed in XPS after 60 min exposure to NH_3 ($\sim 10^{14}$ molecules $\text{cm}^{-2} \text{s}^{-1}$) and 5.0 eV photons (1.5×10^{16} photons cm^{-2} , 50 Hz) at 400 K.

B. Structure and reactivity of surface nitrides

Having presented XPS evidence for surface nitride formation, we now examine the structure and reactivity of these surface nitrides. In the following, we will simply refer to the process of exposing the GaAs(100)-(4×6) to NH_3 ($\sim 10^{14}$ molecules $\text{cm}^{-2} \text{s}^{-1}$) and 6.4 eV photons (193 nm) (5×10^{15} photons cm^{-2} , 50 Hz) at 102 K for 60 min as *nitridation*. Figure 2 shows three N (1s) XP spectra taken at 102 K after nitridation and heating momentarily to the indicated temperatures. With no heating, spectrum (a) is identical to spectrum (b) in Fig. 2 and the three

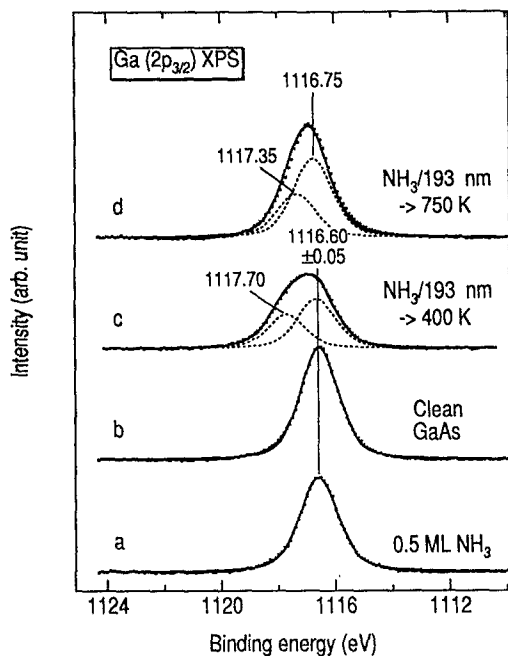


FIG. 3. Ga($2p_{3/2}$) x-ray photoelectron spectra (XPS) taken at 102 K for (a) 0.5 ML NH_3 on GaAs(100)-(4 \times 6) at 102 K; (b) clean GaAs(100)-(4 \times 6); the GaAs surface exposed to NH_3 ($\sim 1 \times 10^{14}$ molecules/cm 2 s) and 193 nm light (5 mJ/cm 2 pulse, 50 Hz) for 60 min at 102 K and heated to 400 K (c) and 750 K (d), respectively. The solid curves are overall fits to the experimental data (dots) while dashed curves are deconvoluted peaks (see text).

deconvoluted peaks are assigned to GaN (397.0 eV), $\text{NH}_x\text{-AsN}$ (~ 398.5 eV) and negligible amounts of NH_3 (400.1 eV). Heating the NH_3 photon exposed GaAs(100) surface to 400 K (b) results in a slight depletion of the 398.5 eV peak, a result of a small amount of recombinative NH_3 desorption from NH_x ($x=1,2$), as observed in temperature programmed desorption (see below). Further flashing to 750 K removes the peak at 398.5 eV. This is due to the recombinative NH_3 desorption of NH_x species and the thermal desorption of AsN, as shown below in AsN TPD. The resulting spectrum (c) can be fit with a single mixed-Gaussian-Lorentzian function (solid line) peaked at 396.6 eV with a FWHM of 1.9 eV. While the intensity of the GaN peak remains unchanged between 100 and 750 K, the N ($1s$) binding energy for GaN in spectrum (d) is 0.4 eV lower than those in spectra (b) and (c), possibly due to the desorption of arsenic nitride, which changes the local electronic structure of GaN.

Accompanying the above changes in N ($1s$) XPS, Ga and As core level XP spectra provide complementary information. Figure 3 shows a set of Ga ($2p_{3/2}$) XP spectra taken at 102 K for (a) 0.5 ML NH_3 covered GaAs(100)-(4 \times 6); (b) clean GaAs(100)-(4 \times 6); (c) the GaAs(100)-(4 \times 6) surface exposed to NH_3 and 6.4 eV photons at 102 K, and heated momentarily to 400 K; (d) the above nitride-covered surface heated to 750 K. For both the clean and 0.5 ML NH_3 covered GaAs(100)-(4 \times 6) surfaces, the Ga ($2p_{3/2}$) spectra can be fit with a single mixed-Gaussian-Lorentzian function (solid line)

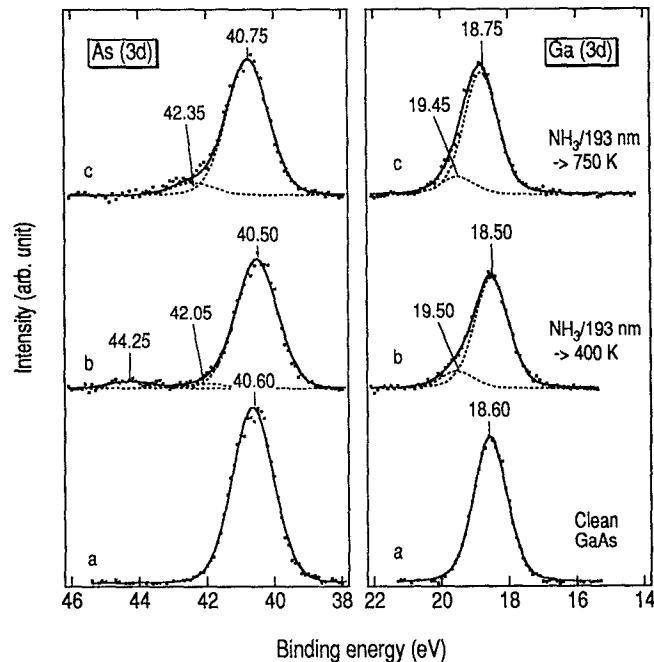


FIG. 4. As($3d$) (left panel) and Ga($3d$) (right panel) x-ray photoelectron spectra (XPS) taken at 102 K for, from bottom to top, the clean GaAs(100)-(4 \times 6) surface, the GaAs surface exposed to NH_3 ($\sim 1 \times 10^{14}$ molecules/cm 2 s) and 193 nm light (5 mJ/cm 2 pulse, 50 Hz) for 60 min at 102 K and heated to 400 and 750 K, respectively. The solid curves are overall fits to the experimental data (dots) while dashed curves are deconvoluted peaks (see text).

peaked at 1116.60 ± 0.05 eV with a FWHM of 1.6 eV. This Ga peak can be assigned to substrate GaAs. Compared to the clean surface, the Ga ($2p_{3/2}$) intensity is attenuated by 16% upon saturation NH_3 adsorption at 102 K. This can be used to calibrate the absolute ammonia coverage, as shown below (Sec. III C).

After the nitridation process at $h\nu=6.4$ eV, with or without subsequent heating to 400 K, the Ga($2p_{3/2}$) XPS shows a broad peak which can be deconvoluted, with FWHM of 1.6 eV, into two peaks at 1116.60 ± 0.05 and 1117.70 eV, respectively. The former is from substrate GaAs while the latter can be assigned to surface Ga nitride. Further heating of this surface to 750 K results in an increase in the substrate Ga intensity, as expected for the desorption of surface As nitrides which attenuate the substrate Ga peak intensity at lower surface temperatures. The slight increase (+0.15 eV) in the substrate Ga ($2p_{3/2}$) binding energy may be due to minor changes in surface band bending, which can change the Fermi level position.⁶ Interestingly, while the intensity of the surface Ga nitride peak remains constant upon heating from 400 to 750 K, its binding energy is decreased by 0.35 eV. This change is coincident with the decreased N ($1s$) BE for surface Ga nitride (Fig. 2). Similar changes can be found in the Ga and As ($3d$) regions, shown in Fig. 4.

The right panel in Fig. 4 shows three Ga ($3d$) XP spectra taken at 102 K for: (a) clean GaAs(100)-(4 \times 6); (b) the GaAs surface exposed to NH_3 and 6.4 eV photons at 102 K, and heated momentarily to 400 K; and (c) the

above nitride-covered surface heated to 750 K. For clean GaAs(100)-(4×6), the Ga (3*d*) spectra can be fit with a single mixed-Gaussian-Lorentzian function (solid line) peaked at 18.60 eV with a FWHM of 1.2 eV. Similar to the Ga (2*p*) XP spectra, nitridation leads to the appearance of a Ga (3*d*) peak at 19.50 eV, which is 1.00 eV higher than the substrate peak at 18.50 eV. The slight shift (± 0.15 eV) of the bulk Ga (3*d*) peak can again be attributed to changes in the Fermi level due to band bending. Referenced to the substrate Ga (3*d*) peak position (18.60 ± 0.15 eV), the chemical shift of the Ga nitride species decreases from 1.00 to 0.70 eV when the nitride-covered surface is heated from 400 to 750 K, in agreement with the Ga (2*p*) spectra in Fig. 3.

The corresponding As (3*d*) spectra are shown in the left panel in Fig. 4. For the clean GaAs(100)-(4×6) surface, the As (3*d*) peak can be fit with a single mixed-Gaussian-Lorentzian function (solid line) peaked at 40.60 eV with a FWHM of 1.4 eV. Nitridation of the surface at 102 K and heating to 400 K, leads to the appearance of a peak at 44.25 eV, which is 3.75 eV higher than the BE for substrate As. We assign this peak to surface As nitrides. Heating the nitride covered surface to 750 K removes the peak at 44.25 eV. This, along with Fig. 2 and the TPD results presented below (Fig. 5), suggests the desorption of surface As nitrides upon heating to 750 K. Interestingly, a new As (3*d*) peak at 42.35 eV, 1.60 eV higher than the BE for substrate As, appears when the surface is heated to 750 K. The appearance of this new As (3*d*) peak is accompanied by decreased binding energies for N (1*s*), Ga (2*p*), and Ga (3*d*) for Ga nitrides (Figs. 2–4). We believe these changes are due to the formation of new nitride species, possibly involving the insertion of N to the Ga–As back bonds.

The desorption of surface As nitrides can be directly followed by temperature programmed desorption (TPD) mass spectroscopy. Figure 5 shows the TPD spectra for four masses, $m/e=69$ (Ga^+), 75 (As^+), 83 (GaN^+), and 89 (AsN^+), taken after a GaAs(100)-(4×6) surface was exposed simultaneously to NH_3 and 6.4 eV photons at 102 K. While GaN shows no detectable thermal desorption signal, AsN desorbs between 600 and 800 K, with a peak at 750 K. The As^+ ($m/e=75$) spectrum tracks that of AsN^+ and is assigned to the mass spectrometer cracking signal of AsN. The Ga^+ signal above 800 K is due to the sublimation of atomic gallium. The desorption of other As containing species was not observed. In addition to the above products, the presence of some surface NH_x ($x=1,2$) species also gives rise to a small amount of NH_3 and H_2 desorption between 300 and 700 K. Unfortunately, the relatively high NH_3 exposure in the nitridation experiment results in high background interference for the NH_3 and H_2 TPD spectra (not shown). Details on NH_3 and H_2 desorption will be presented more clearly in Sec. III D.

Figure 6 compares the high resolution electron energy loss spectra of clean and nitride covered GaAs(100) surfaces. All spectra are normalized to their elastic peak intensities. The elastic peak intensities of nitride covered surfaces are 20 to 30 times lower than that of the clean

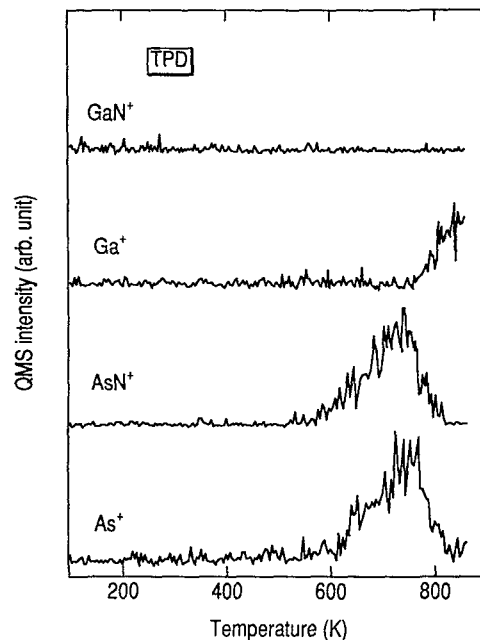


FIG. 5. Temperature programmed desorption (TPD) spectra (from bottom to top, $m/e=75$, 89, 69, and 83 for As^+ , AsN^+ , Ga^+ , and GaN^+ , respectively) taken after the GaAs(100)-(4×6) surface was exposed simultaneously to NH_3 ($\sim 1 \times 10^{14}$ molecules/ cm^2 s) and 6.4 eV photons (5 mJ/ cm^2 pulse, 50 Hz, incident at 60° off surface normal) for 60 min at 102 K.

GaAs(100)-(4×6) surface, indicating significant roughening of the surface upon nitridation. Confirming this, LEED shows (1×1) diffused spots corresponding to substrate fundamentals and high background, indicating a somewhat disordered and roughened surface.

For the clean GaAs surface, the HREEL spectrum (a) is dominated by surface optical phonons at 288 cm^{-1} (ν_p) and 576 cm^{-1} ($2\nu_p$), respectively. Nitridation at 102 K [spectrum (b)] results in additional losses at 598, 800, 1070, 1510, 1610, and 3330 cm^{-1} , respectively. As shown in more detail in Sec. III E, the losses at 3330 and 1510 cm^{-1} are the stretching, $\nu_s(\text{NH})$, and deformation, $\delta_s(\text{HNN})$, of surface NH_2 groups. The losses at 1070 and 1610 are assigned to the accumulation of some background H_2O during the long experimental time.¹⁶ Compared to the clean surface spectrum (a), the intensity of the 598 cm^{-1} peak cannot be solely accounted for by the phonon loss ($2\nu_p$). We assign the losses at 598 and $\sim 800 \text{ cm}^{-1}$ to the stretching vibration of surface Ga–N and As–N species. Heating the nitride covered surface to 400 K [spectrum (c)] removes the features due to background water and the spectrum is dominated by losses assigned to Ga and As nitrides (598 and $\sim 800 \text{ cm}^{-1}$, respectively) and surface NH_2 group (1510 and 3320 cm^{-1}). Further heating to 700 K [spectrum (d)] removes the loss peak at 800 cm^{-1} , as expected for the desorption of surface As nitrides. The dominant feature is a broad peak between 500 and 800 cm^{-1} , corresponding to the overlapping vibrational frequencies of surface GaN. For comparison, the vibrational modes of single crystal GaN are at 560 and 744 cm^{-1} ,

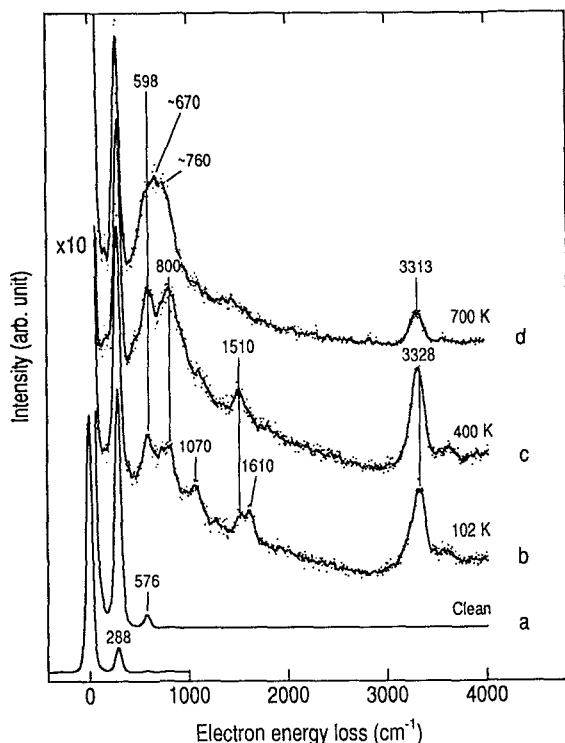


FIG. 6. HREELS for (a) clean GaAs(100)-(4×6); (b) the GaAs surface exposed to NH₃ (~1×10¹⁴ molecules/cm²s) and 193 nm light (5 mJ/cm² pulse, 50 Hz) for 60 min at 102 K (b), and heated to 400 K (c) and 700 K (d), respectively. All spectra were taken at 102 K with a primary electron energy of 3 eV and a resolution (FWHM) of 70 cm⁻¹. Each spectrum was normalized to its elastic peak intensity. The loss region of all spectra were multiplied by a factor of 10 with respect to the elastic peak.

respectively.¹⁷ Finally, heating to 700 K shows, in addition to the nitride losses, $\nu_s(\text{NH})$, but no $\delta_s(\text{HNH})$, in the HREEL spectrum (d). The absence of the $\delta_s(\text{HNH})$ mode indicates that the N-H stretch at 3313 cm⁻¹ is not due to surface NH₂. As discussed in more detail in Sec. III F, this $\nu_s(\text{NH})$ loss at 3313 cm⁻¹ is from the surface NH group.

We have also taken HREEL spectra (not shown) after nitridation at $h\nu=5.0$ eV and found that the dominant surface species is NH₂. Loss features for nitrides are much weaker than those in Fig. 6, indicating a much slower photochemical nitridation rate, in agreement with XPS results presented in Fig. 1.

The above results show conclusively that Ga nitride, As nitrides, and surface NH₂ groups are formed on GaAs(100)-(4×6) at 102 K by simultaneous exposure to NH₃ and uv photons. While gallium nitride is thermally stable, surface arsenic nitride desorbs between 600 and 800 K. In the following, we turn to surface coverage calibration and the mechanism of photoassisted nitridation.

C. Surface coverage calibration

The absolute coverage of ammonia on GaAs(100)-(4×6) can be obtained from the relative intensity for N (1s) and Ga (2p_{3/2}) XPS transitions, as well as from the

relative attenuation of substrate Ga (2p_{3/2}) XPS intensity upon ammonia adsorption. The latter is given by^{18(a)}

$$\frac{I_{\text{Ga}}(\text{NH}_3)}{I_{\text{Ga}}(\text{clean})} = 1 - \theta_{\text{NH}_3} + \theta_{\text{NH}_3} \cdot \exp\left\{-\frac{a_{\text{NH}_3}}{\lambda_{\text{Ga}}}\right\}, \quad (1)$$

where a_{NH_3} is the effective size of the adsorbed NH₃ and can be approximated by the diameter of the nitrogen atom, ~2 Å. For Ga (2p_{3/2}) photoelectrons, the kinetic energy is ~130 eV, and λ_{Ga} , the escape depth, is 5 Å.¹⁸ Based on the measured attenuation of XPS intensities, $I_{\text{Ga}}(\text{NH}_3)/I_{\text{Ga}}(\text{clean})=0.84$, Eq. (1) gives a saturation ammonia coverage of 0.5 ± 0.1 ML (NH₃ to surface atom ratio), or $3.2 \pm 0.6 \times 10^{14}$ molecules/cm².

The NH₃ coverage can also be calculated independently using the relative intensities of N (1s) and substrate Ga (2p_{3/2}). For a clean GaAs(100)-(4×6) surface, the intensity of the Ga (2p_{3/2}) transition is given by^{18(a),19}

$$I_{\text{Ga}}(\text{clean}) = I_{\text{Ga}}^0 \frac{\{(1-x_{\text{Ga}}) + x_{\text{Ga}} \cdot \exp(-b/\lambda_{\text{Ga}})\}}{1 - \exp(-d/\lambda_{\text{Ga}})}, \quad (2)$$

where $x_{\text{Ga}}=0.7 \pm 0.1$ ML, the fractional Ga coverage of the Ga-rich surface,^{11,19} $b=1.41$ Å and $d=2.83$ Å are the interlayer distances of the As-Ga and Ga-Ga layers, respectively, for the GaAs(100) face. I_{Ga}^0 is proportional to the sensitivity factor for Ga(2p_{3/2}). Since all the N (1s) signal is from the top adsorbate layer, the intensity for N (1s) is simply given by

$$I_{\text{N}} = I_{\text{N}}^0 \theta_{\text{NH}_3}, \quad (3)$$

where I_{N}^0 is proportional to the sensitivity factor for N (1s). From the measured ratio of XPS intensities, $I_{\text{N}}/I_{\text{Ga}}(\text{clean})$, and the known ratio of sensitivities factors, $I_{\text{N}}^0/I_{\text{Ga}}^0=0.055$,^{18(b)} Eq. (2) gives a saturation ammonia coverage of 0.44 ± 0.09 ML, within the error range given by Eq. (1). Similarly, the coverages of N containing species after nitridation can be obtained.

D. Photodissociation of chemisorbed ammonia: Kinetics

The low ammonia flux used in the nitridation process assures insignificant gas phase absorption at 6.4 eV. Nitridation must occur at the adsorbate-substrate interface because of the photon energy and substrate temperature dependence presented in Sec. III A. To probe the mechanism, we studied the photolysis of *preadsorbed* ammonia. In these experiments, a saturation amount of ammonia (0.5 ± 0.1 ML) is adsorbed on the GaAs(100)-(4×6) surface at 102 K. The ammonia covered surface is then irradiated with uv photons. Analysis is done by following the time-of-flight (TOF) distribution of photodesorbing products during irradiation and by monitoring the surface species after irradiation (TPD, HREELS, XPS). We first probe the kinetics of ammonia photolysis.

Figure 7 shows a set of ND₃ (left panel) and D₂ (right panel) TPD spectra taken after 0.5 ML ND₃ was irradiated at 102 K with various amounts of 6.4 eV photons. ND₃ and D₂ are the only detectable thermal desorption

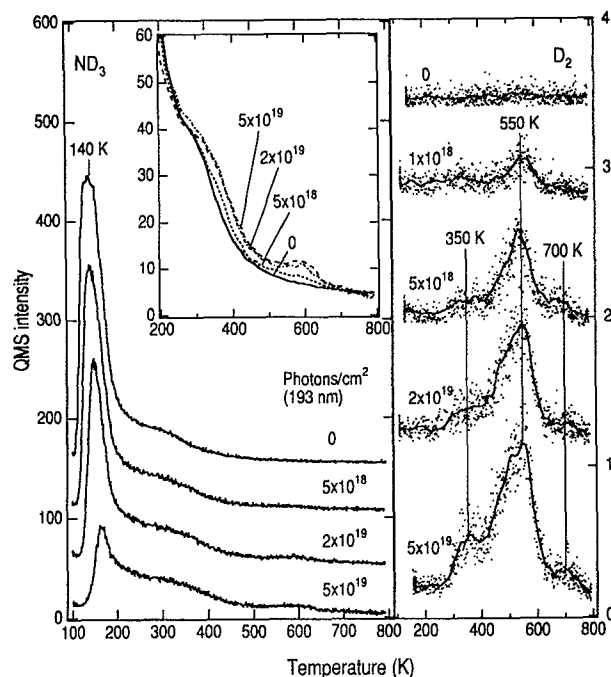


FIG. 7. Temperature programmed desorption (TPD) spectra ($m/e=20$ in the left panel and $m/e=4$ in the right panel) taken after 0.5 ML ND_3 covered $\text{GaAs}(100)-(4\times 6)$ was irradiated at 102 K by the indicated number of 6.4 eV (193 nm) photons. The inset shows the smoothed and expanded ND_3 signal in the 200–800 K region. Please note the different intensity scale for the two panels.

products below 800 K. Above 800 K, the sublimation of both Ga and As occurs. For 0.5 ML ND_3 with no irradiation, the ND_3 TPD spectrum is characterized by a major peak ($\sim 75\%$) at 140 K and a minor shoulder ($\sim 25\%$) between 200 and 400 K. At lower ND_3 coverages (not shown), only the high temperature state is populated. Using Redhead analysis and assuming first order desorption kinetics, we obtained a desorption activation energy of ~ 0.8 eV at very low coverages (<0.05 ML) and ~ 0.35 eV for the main desorption peak at high coverages. There is no kinetic isotope effect in TPD spectra.

For 0.5 ML ND_3 -GaAs, with increasing irradiation, the area of the 140 K desorption peak decreases, while the shoulder shows no significant change. As shown below, the depletion of ND_3 is mainly due to molecular ND_3 photodesorption, but there is a small amount of photodissociation. A careful examination of the region ≥ 200 K shows interesting changes (inset in Fig. 7). In contrast to the major desorption peak at 140 K, the amount of ND_3 desorption in the region ≥ 250 K increases with photon fluence and a small new desorption peak at ~ 600 K emerges. These additional features are assigned to the recombinative desorption of photochemically formed ND_x ($x=1,2$) species. Further support of this assignment will be presented later in Sec. III E.

The right panel in Fig. 7 shows a set of D_2 TPD spectra taken following ND_3 adsorption and irradiation. Without irradiation, no D_2 thermal desorption was observed, as expected for the absence of ammonia thermal decomposi-

tion. Photoirradiation leads to the appearance of a D_2 TPD peak at 550 K. This peak, along with two less intense peaks at 350 and 700 K, grows with the extent of photolysis. These D_2 TPD peaks result from the thermal dissociation of photochemically formed ND_2 on the surface (see below). The intensity of the D_2 desorption is more than two orders lower than that for ND_3 in the left panel. From the QMS sensitivity factors for D_2 and ND_3 , we estimated that the D_2 desorption in the right panel accounts for $\sim 10\%$ of the loss of molecular ND_3 in the left panel, indicating that the photodissociation cross section is about one order lower than that for photodesorption. Similar results (not shown) are obtained for $h\nu=5.0$ and 3.5 eV (248 and 351 nm).

In D_2 TPD measurements, the ND_x ($x=1-3$) covered GaAs sample was heated to 250 K before it was positioned in front of the QMS ionizer. We found this procedure was necessary because a small amount of electron (from the QMS filament) induced dissociation of adsorbed ND_3 interfered with the quantitative assessment of photodissociation. Without the above heating procedure, a test experiment for 0.5 ML of ND_3 covered surface at 102 K showed a small amount of D_2 thermal desorption, with an intensity equivalent to the second (from top) D_2 TPD spectrum in the right panel of Fig. 7. Since heating the surface to 250 K desorbs the majority of surface ND_3 , electron damage becomes insignificant, as evidenced by the absence of D_2 desorption in the topmost spectrum in the right panel of Fig. 7. Interestingly, a recent report by Singh *et al.* suggested a small amount of thermal dissociation for NH_3 on the Ga-rich $\text{GaAs}(100)-(4\times 1)$ surface.²⁰ It is likely that electron-induced dissociation might play a role in the above study.

The coverages of ND_3 (ML) and D_2 (uncalibrated) as a function of photon fluence are presented in Fig. 8 for three photon energies, $h\nu=6.4$ (open squares), 5.0 (open triangles), and 3.5 eV (solid circles). The D_2 TPD area in the upper panel increases with photon fluence within the range studied, except for $h\nu=6.4$ eV, where it saturates at 5×10^{19} photons/cm² and decreases with higher fluence. This decrease is attributed to the photolysis of surface ND_2 groups.

For ND_3 , lower panel, the coverage decreases monotonically with photon fluence at all three photon energies. The decrease can be fit with single exponentials (dotted, dashed, and solid lines for 6.4, 5.0, and 3.5 eV, respectively) that give overall first-order photolysis cross sections for 0.5 ML ND_3 -GaAs(100)-(4 \times 6) at three photon energies: $\sigma_{6.4\text{ eV}}=1.3\pm 0.1\times 10^{-20}$ cm², $\sigma_{5.0\text{ eV}}=3.4\pm 0.4\times 10^{-21}$ cm², and $\sigma_{3.5\text{ eV}}=4.0\pm 0.5\times 10^{-21}$ cm². Because the N-D dissociation cross sections are more than one order lower, these values can be taken as the photodesorption cross sections. With the above photodesorption cross sections and the initial slope of the D_2 increase in the upper panel, we estimated the initial ND_3 photodissociation cross sections: $\sigma_{\text{dis}}(6.4\text{ eV})\approx 1\times 10^{-21}$ cm², $\sigma_{\text{dis}}(5.0\text{ eV})\approx 1\times 10^{-22}$ cm², and $\sigma_{\text{dis}}(3.5\text{ eV})\approx 1\times 10^{-22}$ cm².

In an attempt to differentiate the photodesorption and

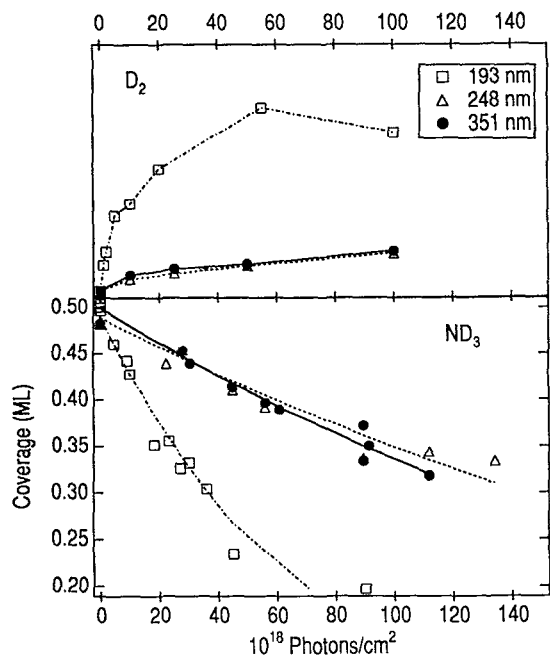


FIG. 8. Post-irradiation TPD areas for D_2 (upper panel) and ND_3 (lower panel, ML) as a function of photon fluence for 0.5 ML ND_3 -GaAs(100)-(4 \times 6) at three light wavelengths (open squares, 193 nm; open triangles, 248 nm; solid circles, 351 nm). The data points were from TPD spectra like those in Fig. 7. The lines (dot-dashed, 193 nm; dashed, 248 nm; solid, 351 nm) in the lower panel are exponential fits for simple first order kinetics.

dissociation channels more quantitatively, we have monitored the concentration of N-containing species following ammonia adsorption and photoirradiation by XPS. The inset of Fig. 9 shows a set of N (1s) XP spectra taken at 102 K, following NH_3 adsorption and irradiation with the indicated 6.4 eV photons (from top to bottom: 0, 1×10^{18} , 5×10^{18} , 1×10^{19} , 5×10^{19} photons/cm 2). Photodesorption of N-containing species (NH_3) is evident by the decrease in the N(1s) peak area with increasing photon fluence. This is shown as solid triangles in Fig. 9, along with molecular NH_3 coverage obtained from post-irradiation TPD areas (open circles). Clearly, within experimental error, these two sets of data are identical. The solid line is a least-square fit (semilogarithmic) to the data points at photon fluences $< 2 \times 10^{19}$. This yields a photolysis cross section of $5.4 \pm 0.5 \times 10^{-20}$ cm 2 for 0.5 ML NH_3 -Ga(100)-(4 \times 6) at $h\nu = 6.4$ eV. At photon fluences higher than 2×10^{19} , the data deviate from linearity, possibly due to the small amount of strongly bonded ammonia which has a lower photolysis cross section than the main adsorption state (see TPD results in the left panel of Fig. 7). The difference between the N (1s) and NH_3 TPD areas is also obvious at high photon fluence. At 5×10^{19} photons/cm 2 , while TPD shows 0.15 ± 0.2 ML NH_3 on the surface, XPS indicates 0.20 ± 0.03 ML of N-containing species on the surface. The difference (~ 0.05 ML) accounts for the photodissociation products on the surface. A careful examination of the N (1s) XP spectra shows that, in addition to molecular ammonia at BE=400.1 eV, a component at

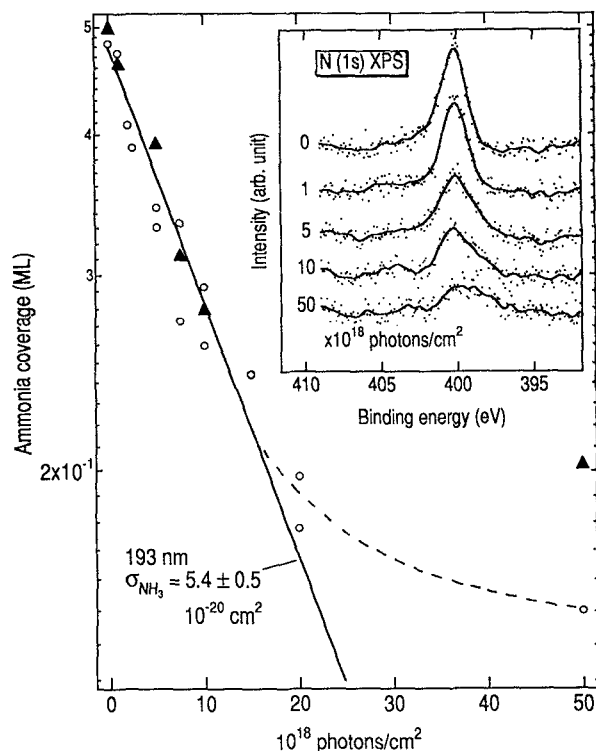


FIG. 9. NH_3 coverage obtained from post-irradiation NH_3 TPD areas (open circles) and N (1s) XPS peak areas (solid triangles) as a function of photon fluence for 0.5 ML NH_3 -GaAs(100)-(4 \times 6) at 193 nm. The inset shows the N (1s) XP spectra taken after 0.5 ML NH_3 -GaAs(100)-(4 \times 6) was irradiated at 193 nm by the indicated number of photons (from top to bottom: 0, 1, 5, 10, and 50 10^{18} photons/cm 2 , respectively).

lower BE (~ 398 – 399 eV), which can be attributed to NH_x ($x=1,2$) species, is evident at high photon fluences ($\geq 1 \times 10^{19}$ photons/cm 2). Due to the relatively low signal-to-noise ratio, deconvolution of the N (1s) XP spectra in the inset of Fig. 9 was not attempted.

The major photolysis channel, molecular photodesorption, can also be followed by time-of-flight spectroscopy. In these experiments, the desorption of molecular ammonia is initiated by a uv laser pulse and is monitored as a function of time with the QMS. For either NH_3 or ND_3 covered GaAs(100)-(4 \times 6), molecular ammonia photodesorption is characterized by a mean translational energy of 52 ± 5 meV or $\langle E_{trans}/2k \rangle = 300 \pm 30$ K, independent of the light wavelength and laser pulse energy. However, the photodesorption yield per laser pulse depends linearly on laser pulse energy in the range studied (0.8–10.5 mJ/cm 2), which clearly points to a *nonthermal* mechanism. The dynamics of molecular ammonia photodesorption, involving a vibration-mediated mechanism, will be presented in detail in the following paper.

E. Identification of surface NH_2 group

The photodissociation products on the surface can be identified spectroscopically using HREELS. We first examine NH_3 saturated GaAs(100)-(4 \times 6) surface with no irradiation. Figure 10 shows a set of HREEL spectra taken following 0.5 ML NH_3 adsorption at 115 K, and heated to

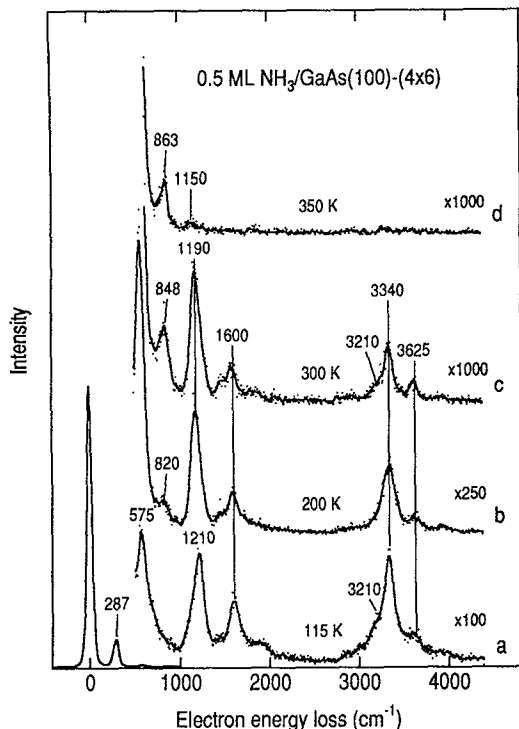


FIG. 10. HREEL spectra for 0.5 ML NH_3 -GaAs(100)-(4 \times 6) at 115 K (a), and heated to 200 K (b), 300 K (c), and 350 K (d), respectively. All spectra were taken at 115 K with a primary electron energy of 3 eV and a resolution (FWHM) of 70 cm^{-1} . Each spectrum was normalized to its elastic peak intensity. The loss region of spectra (a)-(d) are multiplied by 100, 250, 1000, and 1000, respectively.

the indicated temperatures (from bottom to top: 115, 200, 300, and 350 K, respectively). For spectrum (a), 115 K, the adsorbate-related losses are at 1210, 1600, 3210, and 3340 cm^{-1} , and can be assigned to the symmetric-asymmetric deformations and symmetric-asymmetric stretching vibrations of molecular NH_3 , respectively.²¹ The intense losses at 287 (ν_p) and 575 cm^{-1} ($2\nu_p$) are surface optical phonons.²² The weak features on the high frequency side of all losses (ν_i) are phonon overtones ($\nu_i + \nu_p$). These assignments are supported by isotope labeling using ND_3 . Upon annealing to 200 and 300 K, all the positions remain nearly constant, but the intensities decrease significantly (please note the different scaling factors), as expected for molecular ammonia desorption. A new loss feature at 820 cm^{-1} is resolved upon annealing to 200 K (b). Comparing to other NH_3 /substrate systems, we assign this peak at 820 cm^{-1} to surface NH_3 (most likely Ga-NH₃ stretching), although the contribution of NH_3 rocking mode (ρ_r) cannot be unambiguously ruled out. Upon further heating to 300 K (c), this peak shifts slightly to a higher frequency (848 cm^{-1}), which can be attributed to the overlap of the N-surface stretch with the third optical phonon ($3\nu_p$). Finally, heating to 350 K (d), or higher, eliminates all vibrational features assigned to NH_3 and the clean surface spectrum is recovered. The losses at 863 and 1150 cm^{-1} are optical phonons ($3\nu_p$ and $4\nu_p$) of the clean GaAs(100) surface.²² In agreement with

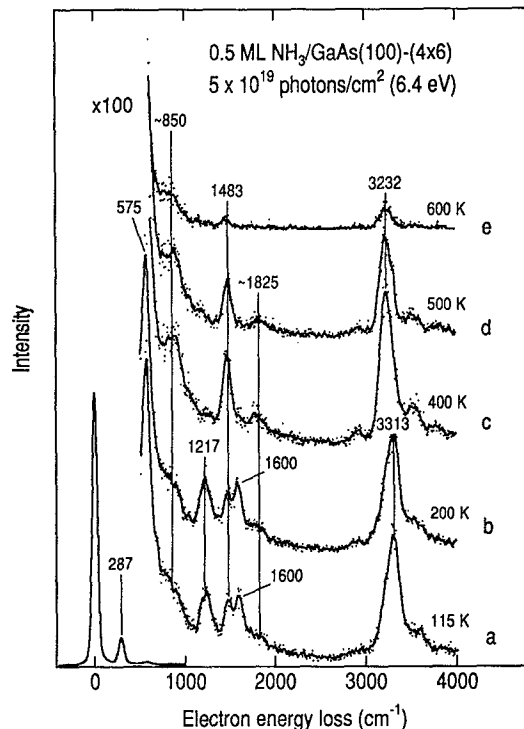


FIG. 11. HREEL spectra taken after 0.5 ML NH_3 -GaAs(100)-(4 \times 6) was irradiated by 5×10^{19} photons/ cm^2 (6.4 eV) at 115 K (a), and heated to 200 K (b), 400 K (c), 500 K (d), and 600 K (e), respectively. All spectra were taken at 115 K with a primary electron energy of 3 eV and a resolution (FWHM) of 70 cm^{-1} . The loss region of all spectra (a)-(d) are multiplied by a factor of 100.

XPS and TPD, the HREELS results in Fig. 10 unambiguously prove that ammonia does not thermally decompose on the Ga-rich GaAs(100) surface.

Figure 11 shows a HREELS annealing set taken after the NH_3 covered surface is irradiated with 5×10^{19} photons/ cm^2 (6.4 eV) at 115 K and annealed to the indicated temperatures. Using HREELS with no heating, spectrum (a) in Fig. 11 shows a new loss peak at 1483 cm^{-1} , in addition to losses assigned to molecular NH_3 . This new loss becomes clearer when the irradiated surface is flashed to 400 K to desorb remaining molecular NH_3 . The resulting spectrum (c) is dominated by losses at 1483 and 3232 cm^{-1} , which are the deformation (δ_s) and stretching vibrations (ν_s) of surface NH_2 .^{21,23,24} The weak shoulder at ~ 850 cm^{-1} cannot be accounted for by the third phonon overtone. [Note the difference in scaling factors for spectrum (d) in Fig. 10 and all spectra in Fig. 11.] It is assigned to the Ga-NH₂ stretch. The broad feature at ~ 1825 cm^{-1} can be deconvoluted to the phonon overtone of $\delta_s(\text{H-NH})$ (1770 cm^{-1}) and $\nu_s(\text{Ga-H})$ (1870 cm^{-1}) for surface hydrogen.²⁵ Further heating of (c) to 500 and 600 K (d) and (e) results in a depletion of all losses assigned to NH_2 . This is a result of the recombinative desorption of NH_3 (g) from NH_2 (a) and H (a), and the thermal dissociation of NH_2 (a) to H_2 (g) (see Fig. 7). Heating above 700 K removes all losses associated with NH_x (not shown). Interestingly, annealing of the NH_2 covered sur-

TABLE I. Vibrational frequencies (cm^{-1}) of ammonia.

Mode	System			
	$\text{NH}_3/\text{GaAs}^a$	$\text{ND}_3/\text{GaAs}^a$	$\text{NH}_3/\text{Ni}(110)^b$	$\text{NH}_3(\text{solid})^b$
$\nu_d(\text{NH})$	3340	2494	3296	3414
$\nu_s(\text{NH})$	3210	2376	NR	3337
$\delta_d(\text{HNNH})$	1600	1176	1616–1728	1646
$\delta_s(\text{HNNH})$	1200	950	1136	1060
$\rho_r(\text{NH}_3)$	NR	NR	600	...
$\nu_s(\text{N-S})$	820	NR	450	...

^aThis work.^bReference 21. NR=not resolved.

face showed no evidence for the formation of a surface NH group, whose bending frequency, $\delta(\text{NH})$, should be lower than that for $\delta_s(\text{HNNH})$.²¹ Similar results have been found for ammonia thermal dissociation on Si surfaces.^{12,13,24}

We have also taken HREEL spectra for ND_3 and isotopically mixed ammonia. The frequencies for ammonia and amido groups are listed in Tables I and II. Interestingly, for isotopically mixed ammonia, the photochemically formed amido groups showed three deformation (scissor mode) frequencies at 1100, 1330, and 1490 cm^{-1} , corresponding to $\delta_s(\text{DND})$, $\delta_s(\text{DNH})$, and $\delta_s(\text{HNNH})$, respectively. This observation unambiguously validates the assignment of amido (NH_2) as the major photodissociation intermediate.

With the above information, we now reexamine the HREEL spectra in Fig. 6 for the GaAs(100) surface exposed simultaneously to NH_3 and 6.4 eV photons. Clearly, the losses at 1510 and 3328 in spectra (b) and (c) are the $\delta_s(\text{HNNH})$ and $\nu_s(\text{NH})$ modes of surface amido. Heating to 700 K eliminates the loss peak at 1510 cm^{-1} for $\delta_s(\text{HNNH})$, but $\nu_s(\text{NH})$ at 3313 cm^{-1} is still present. We assign this $\nu_s(\text{NH})$ at 3313 cm^{-1} in spectrum (d) to surface NH. The intensity of the bending mode for NH may be too weak to be identified, as is the case for NH on Ni(110).²¹ Since the results in Fig. 11 suggest that NH is not formed from the thermal dissociation of NH_2 , we believe that the NH group is formed photochemically at 102 K during the nitridation experiment.

The measured vibrational frequencies of NH_x ($x=2-3$)

TABLE II. Vibrational frequencies (cm^{-1}) of amido groups.

Mode	System			
	GaAs ^a	Ni(110) ^b	Si ^c	NH_2 radical ^d
$\nu_s(\text{NH})$	3232	3280	3388	3337
$\nu_s(\text{ND})$	2420		2483	...
$\delta_s(\text{HNNH})$	1500	1520	1534	1646
$\delta_s(\text{HND})$	1330			...
$\delta_s(\text{DND})$	1100	NR	1157	1060
$\nu_s(\text{N-S})$	850	504	827	...

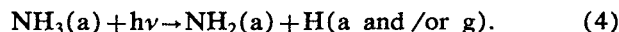
^aThis work.^bReference 21.^cReference 24.^dReference 23.

on GaAs(100)-(4×6) are listed in Tables I and II, along with literature values for other surfaces.

IV. DISCUSSION

A. Chemical pathways for photodissociation and nitridation

We conclude from all the results presented in Sec. III that the photochemical nitridation process is a result of the photodissociation of adsorbed ammonia. The first step is obviously the formation of the amido group from adsorbed ammonia,



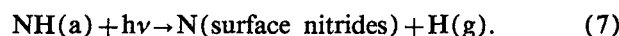
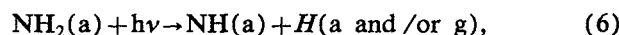
While the Ga-H species was indeed observed spectroscopically following irradiation of monolayer NH_3 covered GaAs(100) (Fig. 11), we do not know whether this pathway is exclusive. It is possible that some H atoms desorb during the photodissociation of adsorbed ammonia. Our previous study showed that the surface Ga-H species is also photoactive,



with a cross section of $1.6 \times 10^{-21} \text{ cm}^2$ at 193 nm.²⁵ Therefore, whatever the detailed pathway, the overall photoreaction should include the desorption of hydrogen. Unfortunately, due to the low photolysis cross section, we were unable to detect hydrogen photodesorption directly.

The post-irradiation HREELS results for monolayer ammonia in Fig. 11 showed no evidence of surface NH group. Low-concentrations of NH species may not be visible in Fig. 11, because the bending mode for NH may be inactive in HREELS, as is the case for NH on Ni(110).²¹ Heating the NH_2 covered surface leads to NH_3 and H_2 desorption (Figs. 7 and 11), but no evidence of NH production is found. The convincing evidence for NH as a photodissociation-nitridation intermediate can be found in Fig. 6. The absence of the $\delta_s(\text{HNNH})$ mode at $\sim 1500 \text{ cm}^{-1}$ in spectrum (d) suggests that the $\nu_s(\text{NH})$ mode at 3313 cm^{-1} is not from NH_2 , but from surface NH. Supporting this, we note that the intensity ratio of $\nu_s(\text{NH})-\delta_s(\text{HNNH})$ is about four for spectra (b) and (c) in Fig. 6, but only two for the corresponding spectra (a)-(d) in Fig. 11. This is expected because the $\nu_s(\text{NH})$ intensity at 3328 cm^{-1} in spectra (b) and (c) in Fig. 6 is the sum of NH_2 plus NH. The overall photon and NH_3 fluences in the nitridation experiment (Fig. 6) are much higher than those for monolayer photolysis (Fig. 11). This might be the reason why NH is evident in Fig. 6 but not Fig. 11.

Therefore, we believe the second and third steps leading to nitridation are



As shown in Sec. III B, the surface nitrides formed at 102 K consist of a mixture of GaN and volatile As nitrides, which desorb at 750 K. Interestingly, there is a structural or phase change for GaN when the surface is heated to 750

K, as evidenced by XPS results presented in Figs. 2–4. The binding energies of both N ($1s$) and Ga ($2p$) in GaN are decreased by 0.4 eV upon heating from 400 to 750 K (Figs. 2 and 3). A similar chemical shift of -0.3 eV is also observed for Ga ($3d$) in GaN (right panel in Fig. 4). Accompanying this change, an As ($3d$) peak at 1.6 eV higher than substrate As becomes evident. While the exact nature of this change is not understood, an attractive explanation, consistent with all observations, is that the N atoms bonded to surface Ga become incorporated or inserted into the GaAs lattice structure upon heating to 750 K.

B. Photoexcitation mechanism

Having established the chemical pathway of photoassisted nitridation, we now turn to the mechanism of photoexcitation that leads to the observed N–H bond breaking and parent desorption. The photochemistry of gas phase NH_3 has been extensively studied.²⁶ The lowest-energy electronic transition of NH_3 corresponds to a strong absorption band in the region of 170 to 217 nm (7.3 to 5.7 eV), with a progression of symmetric inversion vibration. Photodissociation in this wavelength region, with NH_2 and H as the primary photofragments, is described by a predissociation mechanism. For solid NH_3 ice, the uv absorption is characterized by a sharp original band at 6.4 eV, with the onset blueshifted by 0.5 eV compared to the gas phase absorption threshold.¹⁵

For chemisorbed ammonia on Ga(100)–(4×6), two electronic excitation mechanisms need to be considered: (i) direct excitation via photon absorption by the adsorbed NH_3 , as observed for gas or condensed phase NH_3 ; and (ii) substrate photon absorption followed by the attachment or transfer of photoexcited carriers to the adsorbate. The direct excitation mechanism can be ruled out at $h\nu = 3.5$ eV. Since the vibrational frequencies of molecular ammonia adsorbed on GaAs(100)–(4×6) are very close to those of gas phase or solid ammonia,²¹ i.e., weakly held, it is not physically sensible to assume that the uv absorption threshold of ammonia can be red-shifted by more than 2 eV through adsorption. Therefore, at $h\nu = 3.5$ eV, the initial excitation step must originate in the substrate and most likely involves the attachment of photoexcited substrate electrons, a process similar to gas phase dissociative electron attachment.

In the gas phase, dissociative electron attachment (DEA) of NH_3 leads to $\text{NH}_2 + \text{H}^-$ or $\text{NH}_2^- + \text{H}$ production. The DEA cross section peaked at electron energies of 5.65 and 10.5 eV.^{27(a)} With greater energy resolution, a more recent study showed that the single DEA peak at 5.65 eV consists of vibrational progression of the inversion mode of NH_3 , with the ground anion vibrational level at 4.93 eV and a vibrational energy spacing of 115 meV.^{27(b)} The close similarity between the vibrational progression in the DEA process and that in the uv absorption spectrum was taken as evidence that DEA is a predissociation process similar to photodissociation.

At $h\nu = 6.4$ eV, in addition to substrate-mediated excitation, direct photon absorption by the adsorbate may also

contribute. The latter cannot be conclusively established by the present study. It is important to note that, because the presence of a semiconductor surface introduces new excitation, relaxation, and chemical pathways for the adsorbed molecule, knowledge of the gas-phase photochemistry is often of limited use in photon-assisted surface processing.

C. Implication for GaAs surface passivation and GaN growth

The technological implication of this study can be realized in two areas of device fabrication: GaAs surface passivation and GaN growth. As set forth in the introduction, passivation is a vital step in controlling interface states and fabricating MIS structures. The laser-assisted process offers two advantages over conventional plasma-assisted processes: (i) the simple application in selective-area passivation via direct laser writing; (ii) the elimination of thermal budget and thus unwanted side reactions associated with the nonselective thermal requirements. The second implication is the possibility of laser-assisted low-temperature growth of GaN, which, at present, is hampered by the high-temperature requirement for OMCVD. It is important to note that, while photochemical activation can lower the growth temperature, some thermal activation is still required to achieve the mobility of the deposited N atom. This mobility is necessary for single crystal growth. As demonstrated in Fig. 1, the rate of laser-assisted growth is not detectable at surface temperatures above ammonia thermal desorption under our UHV conditions. This barrier can be overcome when higher pressure is used to maintain a substantial transient concentration of adsorbed NH_3 for GaN growth at a practical rate. Under these conditions, cw light source is much more desirable than pulsed light source to activate *transiently* adsorbed precursor molecules. This is particularly important when adsorbate activation, not gas-phase photon absorption, plays the dominating role.

V. SUMMARY

To summarize, nitridation of the Ga-rich GaAs(100)–(4×6) surface is achieved at 100 K by simultaneous exposure to ammonia and uv photons in a UHV environment. The nitride layer consists of a mixture of GaN and volatile As nitrides. This process is a result of nonthermal photodissociation of adsorbed ammonia. Surface NH_2 is an important intermediate in photodissociation and nitridation.

ACKNOWLEDGMENTS

This work was supported in part by the Science and Technology Center Program of the National Science Foundation, Grant No. CHE-8920120. M. W. acknowledges a Feodor–Lynen research fellowship of the Alexander-von-Humboldt Society.

- ¹E. Yablonovitch, *Science* **246**, 347 (1989).
- ²C. W. Wilmsen, *Physics and Chemistry of III-V Compound Semiconductor Interfaces* (Plenum, New York, 1985).
- ³L. G. Meiners and H. H. Wieder, *Mater. Sci. Rep.* **3**, 143 (1988).
- ⁴S. Fujieda, M. Mizuta, and Y. Matsumoto, *Jpn. J. Appl. Phys.* **27**, L296 (1988).
- ⁵S. J. Pearton, E. E. Haller, and A. G. Elliot, *Appl. Phys. Lett.* **44**, 684 (1984).
- ⁶S. Gourrier, L. Sinit, P. Friedel, and P. K. Larsen, *J. Appl. Phys.* **54**, 3993 (1983).
- ⁷M. W. Ruckman, J. Cao, K. T. Park, Y. Gao, and G. W. Wicks, *Appl. Phys. Lett.* **59**, 849 (1991).
- ⁸(a) H. Okumura, S. Misawa, and S. Yoshida, *Appl. Phys. Lett.* **59**, 1028 (1991); (b) S. Fujieda and Y. Matsumoto, *Jpn. J. Appl. Phys.* **30**, L1665 (1991).
- ⁹S. Nakamura, Y. Harada, and M. Seno, *Appl. Phys. Lett.* **58**, 2021 (1991).
- ¹⁰D. K. Gaskill, N. Bottka, and M. C. Lin, *Appl. Phys. Lett.* **48**, 1449 (1986).
- ¹¹(a) P. Drathen, W. Ranke, and K. Jacobi, *Surf. Sci.* **77**, L162 (1978); (b) D. K. Biegelsen, R. D. Bringans, J. E. Northrup, and L.-E. Swartz, *Phys. Rev. B* **41**, 5701 (1990).
- ¹²(a) L. Kubler, J. L. Bischoff, and D. Bolmont, *Phys. Rev. B* **38**, 13113 (1988); (b) J. L. Bischoff, F. Lutz, D. Bolmont, and L. Kubler, *Surf. Sci.* **251**, 170 (1991).
- ¹³(a) F. Bozso and Ph. Avouris, *Phys. Rev. Lett.* **57**, 1185 (1986); (b) F. Bozso and Ph. Avouris, *Phys. Rev. B* **38**, 3937 (1988).
- ¹⁴M. Grunze, *Surf. Sci.* **81**, 603 (1979).
- ¹⁵N. Nishi, H. Shinohara, and T. Okuyama, *J. Chem. Phys.* **80**, 3898 (1984).
- ¹⁶C. N. R. Rao, *Water*, edited by F. Franks (Plenum, New York, 1972), p. 93.
- ¹⁷A. S. Barker, Jr. and M. Ilegems, *Phys. Rev. B* **7**, 743 (1973).
- ¹⁸(a) G. Ertl and J. Koppers, *Low Energy Electrons and Surface Chemistry* (VCH, Weinheim, 1985); (b) Φ Handbook of XPS (Perkin Elmer Co., Eden Prairie, 1979).
- ¹⁹M. Wolf, X.-Y. Zhu, T. Huett, and J. M. White, *Surf. Sci.* (in press).
- ²⁰N. K. Singh, A. J. Murrell, D. Harrison, and J. S. Foord, *J. Phys.: Condens. Matt.* **3**, S167 (1991).
- ²¹I. C. Bassignana, K. Wagemann, J. Koppers, and G. Ertl, *Surf. Sci.* **175**, 22 (1986).
- ²²H. Luth and R. Matz, *Phys. Rev. Lett.* **46**, 1652 (1981).
- ²³D. E. Milligan and M. E. Jacox, *J. Chem. Phys.* **43**, 4487 (1965).
- ²⁴A. C. Dillon, P. Gupta, M. B. Robinson, and S. M. George, *J. Vac. Sci. Technol. A* **9**, 2222 (1991), and references therein.
- ²⁵(a) X.-Y. Zhu, M. Wolf, T. Huett, J. Nail, B. A. Banse, J. R. Crieghton, and J. M. White, *Appl. Phys. Lett.* **60**, 977 (1992); (b) X.-Y. Zhu, M. Wolf, and J. M. White, *J. Chem. Phys.* **97**, 5868 (1992).
- ²⁶M. N. R. Ashfold, C. L. Bennett, and R. N. Dixon, *Chem. Phys.* **93**, 293 (1985).
- ²⁷(a) T. E. Sharp and J. T. Dowell, *J. Chem. Phys.* **50**, 3024 (1969); (b) K. L. Strockett and P. D. Burrow, *J. Phys. B* **19**, 4241 (1986).